Int. J. Electrochem. Sci., 16 **(2021)** 151010, doi: 10.20964/2021.01.67

International Journal of
ELECTROCHEMICAL
SCIENCE
www.electrochemsci.org

Corrosion Degradation of Two Coating Systems Exposed for Three Years in a Tropical Oceanic Atmospheric Environment

Baihui Shang[1,2,*], *Lunwu Zhang*[1,3], *Yuqin Zhu*[1], *Shuai Wu*[1], *Junpeng Teng*[1], *Qiongyao He*[1,3], *Yan Su*[1,3,*]

[1] Southwest Technology and Engineering Research Institute, Chongqing, 400039, PR China
[2] School of Material Science and Technology, Yingkou Institute of Technology,115014, PR China
[3] Wanning Hainan, Material Corrosion in Atmospheric Environment, National Observation and Research Station, Wanning, 571500, PR China
*E-mail: bhshang12s@alum.imr.ac.cn, suyan71@126.com

Received: 16 September 2020 / *Accepted:* 3 November 2020 / *Published:* 30 November 2020

Two commercial coating systems applied to aluminum alloy screw connections exposed naturally in a tropical oceanic atmospheric environment were studied. The degradation process after different exposure times was analyzed by a series of test methods: visual appearance, color change, gloss loss, Surface FTIR and EIS. Our experimental results indicated that for the screw connection structure, the joint area was not only more susceptible to corrosion, but also increased the inconsistency of the flat area nearby. The protective ability of coating system 1 was superior to that of coating system 2. The effective protective time of coating system 1 was about two years, while the coating system 2 was less than one year.

Keywords: Natural Exposure Test; Coating Systems; Degradation; Protective Ability

1. INTRODUCTION

Organic coatings have a wide range of applications for corrosion protection of metal structures, especially in corrosive environments [1-6]. In engineering applications, the coating system usually consists of multiple layers, including primer, finish, intermediate paint, and anodic oxide layer for some metals substrate such as aluminum. In addition to many natural environmental factors such as temperature, relative humidity, pollutants, and sunlight (especially ultraviolet radiation), the degradation behavior of coating systems under natural exposure is bound to a very complex process [7-10].

To evaluate the protective ability of coating systems, many kinds of research have been conducted in laboratory artificial environments and natural exposure environments. However, the correlation between laboratory tests and the results of natural weathering was often not strong [9, 11-

13]. Although it is time-consuming to obtain degradation data, a natural exposure test can better reflect the degradation performance of a coating system under practical application conditions. Thus, for practical purposes, it is often necessary to study the degradation process of coating systems under natural weathering [8, 10, 14-19]. Momber studied the performance and integrity of protective coating systems for offshore wind power structures under offshore site conditions [8]. Jie Liu studied the degradation behavior and mechanism of a polyurethane coating under atmospheric conditions in the South China Sea and found that the degradation of the coating was caused by the C–N bond rupture due to ultraviolet radiation [10].

Despite several kinds of research have been carried out toward the natural weathering of coating systems, most of these studies were based on flat samples [9, 10, 14]. Unlike flat structures, the joint area of a screw connection is not only more susceptible to corrosion, but may also further increase the complexity and uncertainty of coating degradation in nearby areas [18]. As the screw connection area is usually a weak spot for corrosion, which becomes one of the key factors to reduce the service life of the aircraft structure, it is useful to research the degradation performance of the coating system applied to aluminum alloy screw connections, especially in a natural exposed environment [20, 21]. However, as far as we know, there were relatively few such studies. Thus, the purpose of this paper is to study the corrosion degradation of coating systems applied to screw connection under systematic research.

In the present study, two coating systems exposed for three years in a tropical oceanic atmospheric environment were studied. The tested coating systems are two types of aircraft commercial coatings used for the protection of aluminum alloy aircraft skin structures. The degradation performance of the coating systems was investigated by color change, gloss loss, Fourier transform infrared spectroscopy (FTIR), and Electrochemical impedance spectroscopy (EIS) measurements. The degradation process of the two coating systems was compared. Based on the test results, the degradation uniformity and protective ability of two coating systems applied to aluminum alloy screw connections under tropical offshore platform exposure conditions were discussed and evaluated.

2. MATERIALS AND METHODS

2.1. Materials and specimen preparation

The sample in this study is a screw connection structure with a joint area and a flat area, as shown in Fig. 1. The metal substrate is made of 7B04 aluminum alloy through T74 heat treatment, and the material of the fastener is 30CrMnSiA alloy steel, the main chemical compositions of which are listed in Table 1 and Table 2, respectively. For surface treatment, the aluminum alloy substrate was under anodizing treatment by sulfuric acid.

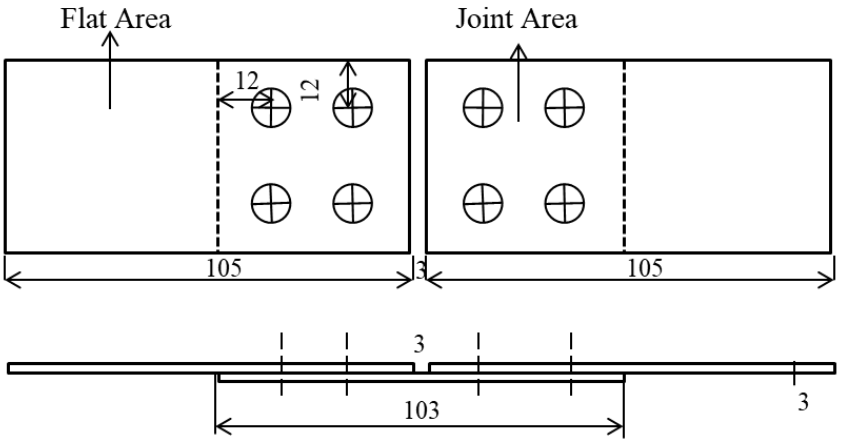

Figure 1. Schematic drawing of the screw connection sample (with scale in mm).

Table 1. Chemical composition of 7B04 aluminum alloy matrix (wt.%).

Element	Si	Cu	Fe	Mn	Mg	Cr	Ni	Zn	Ti	Al
Mass %	≤0.10	1.4~2.0	0.05~0.25	0.20~0.60	1.8~2.8	0.10~0.25	≤0.10	5.0~6.5	≤0.05	Balance

Table 2. Chemical composition of 30CrMnSiA alloy steel fastener (wt.%).

Element	C	Si	Mn	Cr	Ni	Fe
Mass %	0.28~0.34	0.90~1.20	0.80~1.10	0.80~1.10	≤0.030	Balance

Table 3. The main composition of tested coating systems.

System code	Primer Type	Finish Type
Coating 1	Acrylic polyurethane	Fluorinated polyurethane
Coating 2	Epoxy	Polyurethane

Two commercial coating systems, commonly used for aircraft skin were investigated in this study, labeled coating 1 and coating 2. Coating system 1 consisted of Acrylic polyurethane primer and Fluorinated polyurethane finish, while coating system 2 consisted of Epoxy primer and Polyurethane finish, as described in Table 3. The two tested coating systems differed only in composition, and the dry thickness of both coating systems was about 80 μm.

2.2. Methods

2.2.1. Offshore platform exposure

Table 4. Main environment factors at Wanning Test Station

Environment factor	Value
Mean annual temperature (^{o}C)	24.4
Mean annual relative humidity (%)	87
Annual precipitation (mm)	1515.0
Chloride deposition rate (mg/ m^2.d)	38.8
Annual sunshine time (h)	2426.5

The natural weathering test was carried out in Wanning Test Station, located on the east coast of Wanning City, Hainan province of China. The test environment is a tropical marine climate with a typical high corrosion level, as shown by the main environmental factors listed in the table. 4. Natural Exposure tests were facing south with a 45° exposure angle, as shown in Fig. 2. During the exposure, the color change and gloss of the coating surface were measured and recorded at 1, 2, 3, 4, 5, 9, 12, 15, 18, 21, 24, 30, and 36 months. FTIR and EIS tests were carried out to evaluate the corrosion protection ability of the coating system before exposure, and after nature weathering for one, two, and three years.

Figure 2. Physical photo of offshore platform exposure test site

2.2.2. Color change and gloss measurements

During natural exposure, three parallel samples were measured for color change and gloss. A Spectro-guide Color-Guide instrument was applied for color inspection of the coating and the value

ΔE* of color change parameter was calculated. The specular gloss of the coatings at an incident angle of 60° was measured with a PG-1M Gloss Detector, and the rate of gloss loss was calculated.

2.2.3. FTIR measurements

The chemical structure changes in the flat area of the coating surface were studied by FTIR measurement. The spectra were conducted by a Nicolet Nexus 470 Spectrometer (Thermo Electron Corporation, USA), equipped with a diamond ATR unit in the range of 4000–400 cm^{-1}.

2.2.4. EIS measurements

To better evaluate the protective ability of the coating in the flat area at a certain distance from the screw point. a circular region with a diameter of 20 mm in the flat area, with a distance of 40 mm from the nearest fastener was taken as the test area and exposed an approximately 3.14 cm^2 square working area to the solution. For each sample, three similar test spots were selected for EIS measurements.

A self-made fixture type electrolytic cell is used for EIS testing, and the coating on the edge of the sample was polished to maintain an electrical connection. EIS measurements were performed by using a Princeton PARSTAT 2273 electrochemical workstation, and a classical three-electrode system was used in the experiment, with the coated sample acting as the working electrode, a 20 mm × 20 mm platinum plate as counter electrode and the reference electrode was a saturated calomel electrode (SCE). To increase the signal-to-noise ratio, EIS was conducted using an applied AC signal with an amplitude of 20 mV versus the open-circuit potential. The frequency ranged from 10^5 Hz to 10^{-2} Hz at ten points per decade of frequency. Before the test, the sample was immersed in a 3.5wt. % sodium chloride solution for at least 20 minutes to achieve a relatively stable state and the electrochemical experiments were performed in an indoor environment with a temperature approximately 20 °C. The raw data of EIS were fitted by ZsimpWin 3.50 software.

3. RESULTS

3.1. Visual appearance results

The surface appearance of the two coating systems after different times of exposure is shown in Fig. 3.

For coating system 1, as shown in Fig 3a, the overall coating system was in good condition after 1 year of exposure. No apparent change of color in the coating surface was observed, there was no obvious chalking in both the joint area and flat area and no screw corrosion occurred. After 2 years of natural weathering, the images clearly showed that the integrity of the coating was compromised especially in the joint area. More than half of the screws started to corrode. Besides, blisters appeared in the vicinity of the corrosive screws in the joint area, and a small degree of chalking was observed in

the flat area. At the end of the exposure (3 years), the coating system was severely damaged. Almost all screws suffered severe corrosion. The blistering of the coating in the joint area was significant and there was a tendency to spread to the flat area. The average thickness of the coating system in the flat area was slightly reduced to about 75 μm, as a medium degree of chalking was observed on all samples.

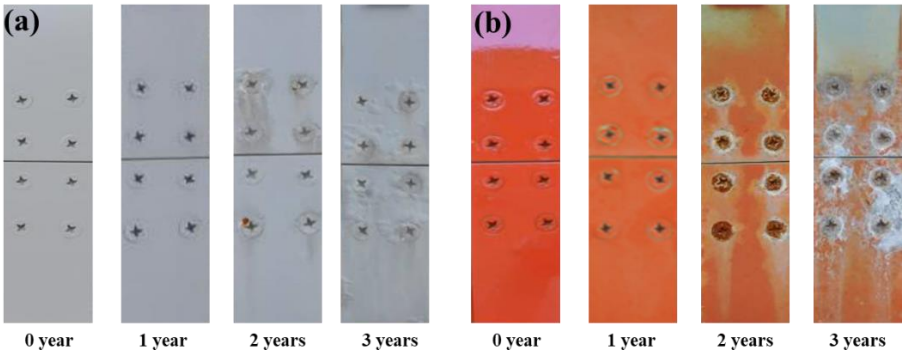

Figure 3. Appearance observed of tested coating systems before and after outdoor exposure with 1, 2, and 3 years (a) coating system 1; (b) coating system 2.

For coating system 2, a large degree of color change and gloss loss could be observed on the coating surface only after one year of exposure, as shown in Fig 3b. As the natural exposure time increased to two years, severe chalking occurred and the orange color of the finish gradually faded away. Almost all screws suffered severe corrosion and loose corrosion products adhere to the screw surface. At the end of the exposure (3 years), the coating system exhibited severe degradation. Parts of the coating in the joint area was almost completely peeled off, and the metal matrix was severely corroded. In the flat area, the orange color of the finish almost disappeared. the average thickness of the coating system was reduced to about 40 μm.

3.2. Color change results

The changes in appearance for the surface of two coatings systems were quite different. To quantize and better understand the appearance change of the coating surface, the color change results before and after different natural exposure times are presented in Fig. 4. The surface color change of coating system 1 was not as obvious as the coating system 2.

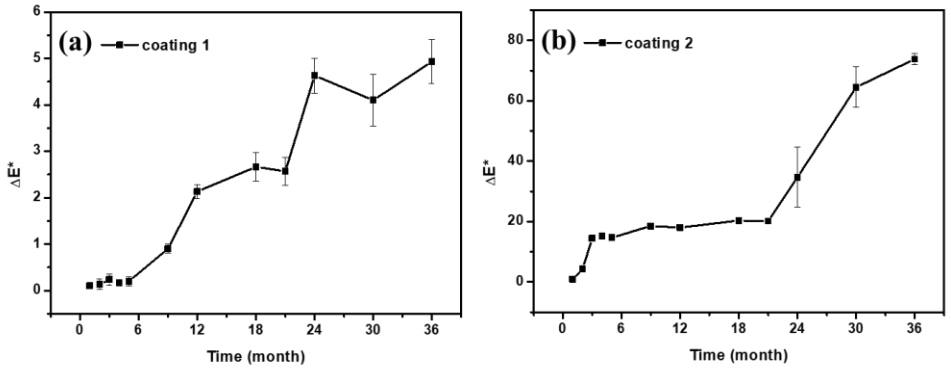

Figure 4. Color change results of tested coating systems before and after outdoor exposure with different time (a) coating system 1 and (b) coating system 2

Fig. 4(a) displayed the color change of coating system 1 under different exposure times. During the first 9 months of exposure, △E* values were all less than 1.5, which means the surface of the finish was generally not discolored. When the natural weathering time increased to 12 ~ 21 months, the coating system showed slight discoloration, with △E* values concentrated in 2 ~ 3. After 24 months of exposure, the △E* values further increased but still less than 5, and the △E* value between 3.1 to 6 indicated that the coating system suffered a slight degree of discoloration [22].

As shown in Fig. 4(b), the surface of coating system 2 had undergone a large degree of color change at a very early time of exposure. Only after 3 months of exposure, did the △E* values exceed 12, indicating a severe degree of discoloration [22]. After two years of exposure, the △E* value further increased rapidly and even reached over 70 at the end of natural weathering. Such a large degree of color change was due to the severe chalking of the coating, which corresponded to the disappearance of the surface orange (Fig. 3(b)) and thinning of the overall thickness of the coating system.

3.3. Gloss loss results

when paint or varnish deteriorates, some holes appear on the surface of the coating, and gradually increase in number and volume. So the coating surface gradually becomes rough, resulting in loss of gloss [10, 11, 23, 24]. Therefore, gloss loss is one of the key factors to evaluate the degradation process of organic coatings and is sometimes used to estimate the service life of organic coatings under service conditions [23]. In general, when the loss of gloss is less than 30%, this stands for a slight degree of gloss loss. It becomes progressive with a value of more than 50%, and it can be considered the coating is tarnished when the value of gloss loss reaches 80% [22].

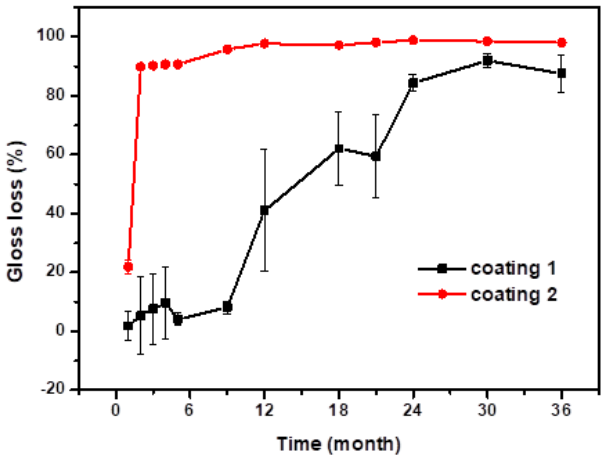

Figure 5. Gloss loss results of tested two coating systems before and after outdoor exposure with different time

Concerning gloss loss results shown in Fig. 5, a similar trend between gloss loss and color change was observed. The gloss loss of coating system 2 increased rapidly and reached about 90% only after only two months of exposure, indicating the gloss of the coating surface was almost completely lost at the beginning of the exposure. With the increase of exposure time, The gloss loss value of coating system 1 gradually increased: less than 30% within the first 9 months of exposure, about 40% to 60% with the exposure time from 12 to 21 months, and over 80% after 24 months of exposure. After 2 years of outdoor exposure, the coating system 1 also suffered severe gloss loss.

3.4. Surface FTIR results

Depending on the amount of infrared radiation absorbed and the particular frequency of major functional groups, infrared spectroscopy is a useful technique for identifying the groups in compounds. Thus, the surface FTIR results can reflect the degradation mechanisms of the coating systems [2, 9, 24, 25].

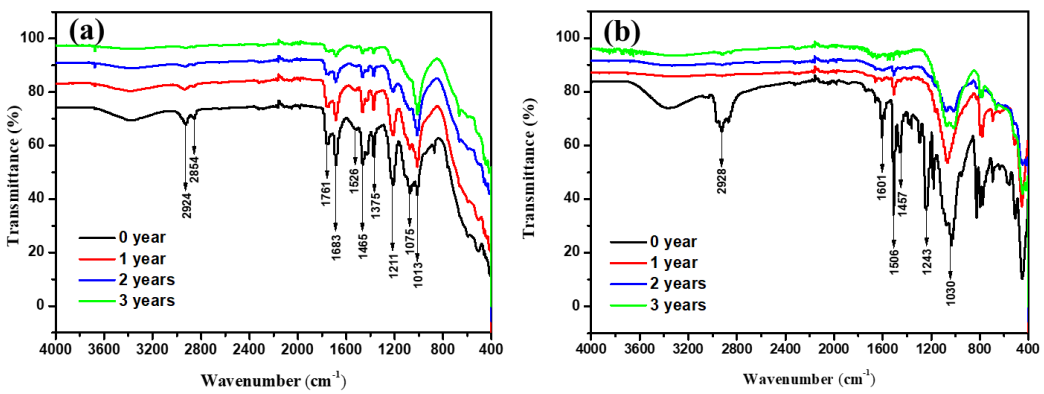

Figure 6. FTIR spectra obtained of tested coating systems before and after outdoor exposure with 1, 2, and 3 years (a) coating system 1 and (b) coating system 2

Table 5. Major IR band attributions of the tested coating systems.

Absorption frequency (cm-1)	Band contribution
2928;2924	vas (-CH_2-)
2854	vs (-CH_2-)
1761;1683	v (C=O)
1601;1506	v (C=C in aromatic rings)
1526	δ (N-H)
1465;1457	δ (-CH_2-)
1375	δ (-CH_3)
1243;1211	v (C-O in ester)
1075	v (C-F)
1030;1011	v (C-O-C)

Fig. 6 shows the surface FTIR results of two coating systems obtained at different times of exposure. The absorption frequencies of major functional groups to the band attribution are summarized in Table 5. The peaks at 2928/2924 cm^{-1} and 2854 cm^{-1} were corresponding to the asymmetric and symmetric stretching vibration of -CH_2- respectively, while the bands of -CH_2- and -CH_3 bending vibration were at 1465/1457 cm^{-1} and 1375 cm^{-1}. The strong peaks at 1761/1683 cm^{-1} and 1243/1211 cm^{-1} were attributed to stretching vibration of C=O and C-O in ester, respectively. It was also obtained bending vibration of N-H at 1526 cm^{-1}. And the peaks at 1601 cm^{-1} and 1506 cm^{-1} could be associated with C=C stretching vibration in aromatic rings, as well as C-F stretching vibration at 1075 cm^{-1}. The peak at 1030/1011 cm^{-1} could be determined by C-O-C stretching vibration [9, 24-26].

Compared to the surface FTIR results before and after a certain period for exposure (Fig. 6), t the peak intensity for major functional groups of both coating systems had occurred to decrease. However, the extent of variation of two coating systems was quite different, indicating the degradation processes of the two coating systems were somewhat different. For coating system 1 (Fig. 6(a)), with the increase of outdoor exposure time, the characteristic peaks such as C=O at 1761/1683 cm^{-1} and C-O in ester at 1211 cm^{-1} gradually decreased, but did not completely disappear even after three years of exposure, indicating that the main functional groups of the fluorinated polyurethane coating were in a process of gradual degradation. For coating system 2 (Fig. 6(b)), only after one year of exposure, a significant change in the chemical composition of the coating could be expected. Except for the peak at 1030 cm^{-1} might be contributed by pigments, almost every peak, such as C=C in aromatic rings at 1601 cm^{-1} and 1506 cm^{-1} disappeared directly. The major functional groups of polymer resin were seriously damaged. A large degree of chalking occurred and small molecule products were gradually taken away by wind and rainfall, resulting in the severe loss of gloss and thickness under natural exposure [10]. Compared with the polyurethane finish, it is obvious that fluorinated polyurethane finish is more resistant to photoaging in the tropical marine atmosphere, as it is widely known that the anti-light aging capabilities of a coating system are mainly reflected in finish.

3.5. EIS results

3.5.1. Impedance modulus at 0.01 Hz

EIS is a powerful quantitative method widely used to study the corrosion behavior of electrode systems [6, 27]. When studying the EIS results for an electrode system, the polarization resistance (R_P: equal to the value of impedance modulus at 0 Hz by definition), an important parameter reflecting the corrosion rate has often been discussed [28]. For complex organic coating systems, some researchers use the impedance modulus at the lowest frequency (usually 0.01 Hz) instead of R_P to evaluate the overall protective ability of the coating system [11, 29, 30].

Fig. 7 shows the Impedance modulus at 0.01 Hz as measured by EIS for tested coating systems after different times of exposure. The $|Z|_{0.01Hz}$ data under each experimental condition were obtained from the same sample at three different test spots in the flat area. Before weathering, the $|Z|_{0.01Hz}$ values were relatively constant, in the order of 10^{10} Ω·cm^2 for coating system 1 and 10^9 Ω·cm^2 for coating system 2, demonstrating the initial coating systems had good uniformity at different test spots. After exposure for a certain time, the $|Z|_{0.01Hz}$ values at different test spots were somewhat different, and the variation trend of the two tested coating systems was different. For coating system 1, the $|Z|_{0.01Hz}$ values varied by about one order of magnitude at different test spots after exposure for one year. The variation further increased by about two and three orders of magnitude, as the $|Z|_{0.01Hz}$ values for different test spots were on the order of (10^8- 10^{10}) Ω·cm^2 and (10^6-10^9) Ω·cm^2 after exposure for two and three years, respectively. For coating system 2, the $|Z|_{0.01Hz}$ values were on the order of (10^5-10^6) Ω·cm^2, 10^7 Ω·cm^2 and (10^5-10^6) Ω·cm^2 with one, two, and three years of exposure, varied by about one order of magnitude at different test spots.

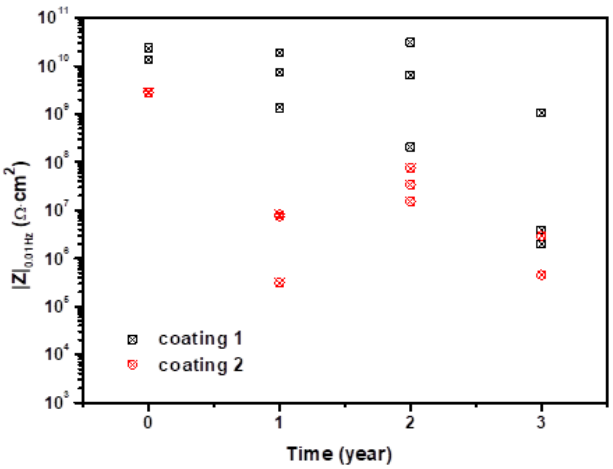

Figure 7. Impedance modulus at 0.01 Hz of tested two coating systems in 3.5 wt.% NaCl solution before and after outdoor exposure with 1, 2, and 3 years

3.5.2. EIS analysis for the test spot with lowest $|Z|_{0.01Hz}$ value

From the previous study, it can be found that for the same test sample, there existed variations in the $|Z|_{0.01Hz}$ values at different test spots. Among these test spots, the test spot with the lowest $|Z|_{0.01Hz}$ value can better represent the weakest part of the coating system in the flat area. Thus, to

investigate the degradation performance of the coating systems under the influence of exposure time, in this section, the EIS result with the lowest $|Z|_{0.01Hz}$ value was typically selected for further analysis and research.

Fig. 8 and Fig. 9 show the typical EIS data in the form of Bode plots for the two tested coating systems after different times of exposure. Different equivalent electrical circuits (EEC), shown in Fig. 10, were used in this study to analyze and quantify the EIS data.

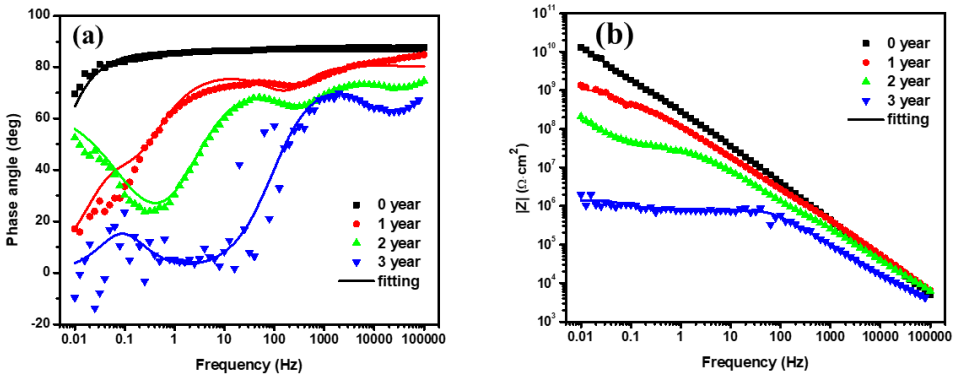

Figure 8. Typical EIS result for coating system 1 in 3.5 wt.% NaCl solution before and after outdoor exposure with 1, 2, and 3 years (a) Bode phase angle plots and (b) Bode impedance modulus plots.

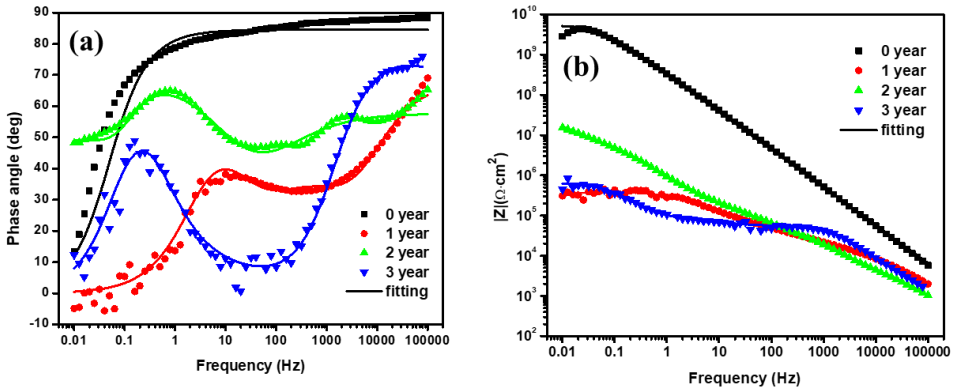

Figure 9. Typical EIS result for coating system 2 in 3.5 wt.% NaCl solution before and after outdoor exposure with 1, 2, and 3 years (a) Bode phase angle plots and (b) Bode impedance modulus plots

Before the outdoor exposure of the sample, the phase angle of the impedance was close to 90° and the logarithm of impedance modulus and frequency was approximately a straight line over a wide frequency range: 10^5-10^{-1} Hz for coating system 1 as well as 10^5-10^0 Hz for coating system 2. The coating system can be viewed as a barrier with large resistance and small capacity. Thus, an EEC with a one-time constant (Fig. 10(a)) was used to fit the EIS data [25, 31]. In this equivalent circle, Rs is the resistance of solution, while Q_c and R_c represent the coating capacity and coating resistance, respectively. Pure capacitance was substituted by a constant phase element (Q) containing two parameters, Y_0, and n to compensate for the non-ideality of the actual electrode system.

After exposure for a while, the electrode process of the coating system became much more complicated, as the combination of the coating deteriorated with the sunlight and corrosive related media such as H_2O, O_2, and Cl^- passed through the coating. A significant drop in impedance modulus had occurred (Fig. 8(b) and Fig. 9(b)) and more than one peaks and troughs appeared in the Bode phase angle plots (Fig. 8(a) and Fig. 9(a)). To better analyzed the coating system, EEC with three time constants (Fig. 10(b)) was applied to fit these EIS data. And in this equivalent circle, the first two time constants Q_1 R_1 and Q_2 R_2 represented the two-layer structure of the coating system, finish, and primer respectively, while the third time constant at the low-frequency region reflect the corroding information of anodized layer and aluminum alloy substrate. Due to the transfer difficulty of corrosive related media to the substrate and/or corrosion products away, a diffusion-controlled reaction sometimes happened following the corrosion process of substrate. Under this circumstance, a Warburg resistance (Z_w) at the low-frequency region was added to the EEC to fit the EIS data, as shown in Fig. 10(c) [32, 33].

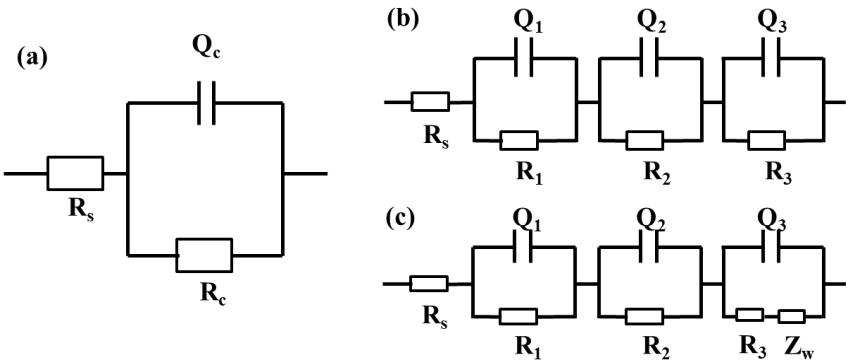

Figure 10. Equivalent electrical circuits (EEC) proposed to fit the EIS data in this study: (a) EEC with one time constant; (b) EEC with three time constants; (c) EEC with three time constants and diffusion characteristic.

In this study, three kinds of equivalent electrical circuits (Fig. 10) were used to fit these EIS data. The fitting data was also shown in straight lines in Fig. 8 and Fig. 9 and the fitting parameters of two coating systems are listed in Table 6 and Table 7, respectively.

Table 6. Fitting parameters of the EIS data for coating system 1 after different exposure times.

Time (year)	Y_{01}/ Y_{0c} ($F\cdot cm^{-2}s^{n-1}$)	R_1/ R_c ($\Omega\cdot cm^2$)	Y_{02} ($F\cdot cm^{-2}s^{n-1}$)	R_2 ($\Omega\cdot cm^2$)	Y_{03} ($F\cdot cm^{-2}s^{n-1}$)	R_3 ($\Omega\cdot cm^2$)	W ($F\cdot cm^{-2}s^{-0.5}$)
0	4.26×10^{-10}	8.20×10^{10}	-	-	-	-	-
1	1.55×10^{-9}	4.24×10^{5}	1.96×10^{-9}	2.77×10^{8}	5.51×10^{-9}	9.46×10^{8}	-
2	2.01×10^{-9}	1.81×10^{3}	2.87×10^{-9}	1.47×10^{5}	3.92×10^{-9}	2.73×10^{7}	7.56×10^{-3}
3	3.80×10^{-6}	6.13×10^{5}	4.94×10^{-9}	8.13×10^{5}	1.19×10^{-8}	8.25×10^{3}	-

4. DISCUSSION

4.1. Degradation uniformity of tested coating systems

With the increase of exposure time, the uniformity of the tested coatings systems was damaged, and the inconsistency of the samples was mainly reflected in two aspects. On the one hand, it showed the difference in coating protective ability between the flat area and the joint area. On the other hand, there were some differences in the degree of coating deterioration in the flat area.

The results in Fig. 3 indicated that the integrity of the coating was compromised in the joint area. Compared with the flat area, the joint area of the samples was more susceptible to corrosion. This result was also supported by Momber [18], as flange connections were critical structural parts in terms of corrosion. Despite adequate coating protection applied to the screws, the joint area was still a relatively weaker area of the whole structure. Water and erosive ions in the atmosphere were more likely to penetrate the coating in this region and eventually induce corrosion and gradually spread to the flat area [18, 20, 21]. Thus, it is useful to perform the local repair at the joint area promptly after corrosion occurred near the screw spot during maintenance, which slowed the expansion of the corrosion to the flat area and delayed large-scale corrosion of the whole structure.

The results in Fig. 7 indicated that there existed differences in the protective ability of the coating system within the flat area, especially for coating system 1. And the variation of $|Z|_{0.01Hz}$ value was about two and three orders of magnitude. After three years of exposure, the protective ability of two test spots was poor while one test spot still maintained good protection. It could be inferred that the joint area of a screw connection was not only more susceptible to corrosion, but also further increased the inconsistency of degradation performance for the coating in the flat area nearby. Therefore, to better evaluate the protective ability of an organic coatings system applied to a connection structure, it is necessary to select the test point at multiple locations.

4.2. Protective ability analysis and evaluation of two tested coating systems

With the increased time of natural weathering, the degradation degree of the two tested coating systems in flat areas was different. For coating system 1, before aging, the overall coating resistance reached a value of 8.20×10^{10} Ω·cm^2 (Table 6), presenting a good protective ability [19]. After one year of exposure, the value of R_1 was 4.24×10^5 Ω·cm^2, indicating the protective ability of finish was almost exhausted. The value of R_2 and R_3 were 2.77×10^8 Ω·cm^2 and 9.46×10^8 Ω·cm^2 respectively, so it can be inferred the primer and anodized layer were still able to provide effective protection for the aluminum alloy substrate. When the weathering time reached two years, the value of R_2 decreased to 1.47×10^5 Ω·cm^2, it can be considered the barrier ability of the primer became poor, while the anodized layer may also be able to provide some protection to the substrate as the value of R_3 was 2.73×10^7 Ω·cm^2. After three years of exposure, the values of R_1, R_2, and R_3 were all below the magnitude of 10^6 Ω·cm^2, as considered the protective ability of the whole coating system was losing [10, 34, 35]. For coating system 2, only after one year of exposure, the values of R_1, R_2, R_3 were all below the magnitude of 10^6 Ω·cm^2, as shown in Table 7, indicating the whole coating system had lost its protective ability. The

values of Y_{01} and Y_{02} were one to two magnitude higher than that of coating system 1 under the same exposure period, the larger values of coating capacity indicating the structure of coating were under greater damaged, further confirmed that the coating system 2 was less resistance to light aging, consistent with the results of FTIR spectra (Fig. 6).

Overall, the protective ability of coating system 1 was better than that of coating system 2, as it was also testified by smaller values of $\triangle E^*$ and gloss loss (Fig. 4 and Fig. 5), as well as larger $|Z|_{0.01Hz}$ values (Fig. 7) with different time of exposure. Our results indicated that the effective protective time of coating system 1 was about two years, while the coating system 2 was less than one year.

5. CONCLUSION

(1) During the natural degradation process of coating systems applied to aluminum alloy screw connection, the joint area of the sample was much more susceptible to corrosion than the flat area.

(2) The joint area of a screw connection could further increase the inconsistency of degradation performance for the coating in the flat area nearby. Therefore, it is recommended to select multiple test points when evaluating the protection ability of the organic coating system for complex connection structures.

(3) The protective ability of coating system 1 was better than that of coating system 2 under natural weathering in a tropical oceanic atmospheric environment. The effective protective time of coating system 1 for the flat area was about two years, while the coating system 2 was less than one year.

ACKNOWLEDGEMENTS
We thanks to the Support of the Introduction of Talent Research Start-up Fund in Yingkou Institute of Technology and the Program for Innovative Research Team in Yingkou Institute of Technology. Miss Jia Zhao is acknowledged for help with FTIR analysis.

References

1. T. Yang, Y. Cui, Z. Li, H. Zeng, S. Luo and W. Li, *J. Hazard. Mater.*, 357 (2018) 475.
2. D. Santos, C. Brites, M.R. Costa and M.T. Santos, *Prog. Org. Coat*., 54 (2005) 344.
3. F. Meng, L. Liu, W. Tian, H. Wu, Y. Li, T. Zhang and F. Wang, *Corrosion Sci.*, 101 (2015) 139.
4. A.A. Younis, W. Ensinger, M.M.B. El-Sabbah and R. Holze, *Mater. Corros*., 64 (2013) 276.
5. S. Liu, L. Liu, F. Meng, Y. Li, F. Wang, *Materials*, 11 (2018) 292.
6. X. Xue and J. Liu, *Int. J. Electrochem. Sci.*, 12 (2017) 3179.
7. A. Momber, *Mater. Corros*., 62 (2011) 391.
8. A.W. Momber, P. Plagemann and V. Stenzel, *Renew. Energ*., 74 (2015) 606.
9. T. Gao, Z. He, L.H. Hihara, H.S. Mehr and M.D. Soucek, *Prog. Org. Coat*., 130 (2019) 44.
10. J. Liu, Z. Li, L. Zhang, J. Hou, Z. Lu, P. Zhang, B. Wang and N. Jin, *Prog. Org. Coat*., 136 (2019) 105310.
11. H. Zhang, Y. Dun, Y. Tang, Y. Zuo, X. Zhao, *J. Appl. Polym. Sci*., 133 (2016) 43893.
12. E. Scrinzi, S. Rossi and F. Deflorian, *Corros. Rev.*, 29 (2011) 275.
13. R. Vera, E. Cruz, M. Bagnara, R. Araya, R. Henríquez, A. Díaz-Gómez and P. Rojas, *Int. J.*

Electrochem. Sci., 13 (2018) 898.
14. A. Lopez-Ortega, R. Bayon, and J. L. Arana, *Materials*, 12 (2019) 1325.
15. S. Zhang, Y. He, T. Zhang, G. Wang and X. Du, *Materials*, 11 (2018) 965.
16. M. Echeverria, C.M. Abreu and C.A. Echeverria, *Corrosion*, 70 (2014) 1203.
17. H. Katayama and S. Kuroda, *Corrosion Sci*., 76 (2013) 35.
18. A.W. Momber, P. Plagemann and V. Stenzel, *Int. J. Adhes. Adhes*., 65 (2016) 96.
19. Z. Li, J. Liu, S. Xing, L. Zhang, Z. Lu and P. Zhang, *Int. J. Electrochem. Sci.*, 15 (2020) 2511.
20. Q. Chen, Z. Cheng, H. Xi, Y. Wang, L. Zhang and G. Liu, *J. Chin. Soc. Corros. Prot*., 27 (2007) 334.
21. L. Zhang, Q. Chen, Y. Wang, Z. Wu, *Eq. Environ. Eng*., 11 (2014) 45.
22. GB/T 1766, Paint and varnishes - Rating schemes of degradation of coats, (2008) China.
23. M. Evans, *Polym. Test*., 31 (2012) 46.
24. G. Gheno, R. Ganzerla, M. Bortoluzzi and R. Paganica, *Prog. Org. Coat.,* 101 (2016) 90.
25. Y. Zhu, J. Xiong, Y. Tang and Y. Zuo, *Prog. Org. Coat*., 69 (2010) 7.
26. Speight, J. G., Lange's Handbook of Chemistry (Sixteenth Edition), McGraw-Hill Professional Publishing, (2004) Columbus, USA.
27. Wang, X., Li H., L. Xu, X. Li, H. Jiang and W. Zhou, *Int. J. Electrochem. Sci.*, 15 (2020) 1450.
28. Y.T. Tan, S.L. Wijesinghe and D.J. Blackwood, *J. Electrochem. Soc.*, 164 (2017) C505.
29. W. Tian, F. Meng, L. Liu, Y. Li and F. Wang, *Sci. Rep.*, 7 (2017) 40827.
30. E. Akbarinezhad, M. Bahremandi, H.R. Faridi and F. Rezaei, *Corrosion Sci*., 51 (2009) 356.
31. X. Yong, Z. Chen, X. Ruan, R. Chen, Y. Fu and Q. Ma, *Prog. Org. Coat*., 136 (2019) 105230.
32. Y. Zuo, R. Pang, W. Li, J.P. Xiong and Y.M. Tang, *Corrosion Sci*., 50 (2008) 3322.
33. J.M. Hu, J.T. Zhang, J.Q. Zhang and C.N. Cao, *Corrosion Sci*., 47 (2005), 47 2607.
34. F.Yang, T. Liu, J.G. Li, S.H. Qiu and H.C. Zhao, *RSC. Adv*., 8 (2018) 13237.
35. J.T. Zhang, J.M. Hu, J.Q. Zhang and C.N. Cao, *Prog. Org. Coat., 49* (2004) 293.